



Ray, Nicola ORCID logoORCID: <https://orcid.org/0000-0001-9645-0812>,
Craig, Chesney ORCID logoORCID: <https://orcid.org/0000-0002-9492-1294>,
Holmes, Paul ORCID logoORCID: <https://orcid.org/0000-0003-0821-3580>,
Rochester, Lynn, Jenkinson, Ned, Brittain, John-Stuart, Grothe, Michel, Silverdale, Monty, Alho, Ana and Alho, Eduardo (2020) Pedunculopontine nucleus microstructure predicts postural and gait symptoms in Parkinson's disease. *Movement Disorders*, 35 (7). pp. 1199-1207. ISSN 0885-3185

Downloaded from: <https://e-space.mmu.ac.uk/625269/>

Version: Published Version

Publisher: Wiley


DOI: <https://doi.org/10.1002/mds.28051>

Usage rights: Creative Commons: Attribution 4.0

Please cite the published version

<https://e-space.mmu.ac.uk>

Pedunculopontine Nucleus Microstructure Predicts Postural and Gait Symptoms in Parkinson's Disease

Chesney E. Craig, PhD,¹ Ned J. Jenkinson, PhD,² John-Stuart Brittain, PhD,³ Michel J. Grothe, PhD,^{4,5} Lynn Rochester, PhD,⁶ Monty Silverdale, MD,⁷  Ana T.D.L. Alho, PhD,^{8,9} Eduardo J.L. Alho, PhD,⁸ Paul S. Holmes, PhD,¹ and Nicola J. Ray, PhD^{1*}

¹Health, Psychology and Communities Research Centre, Department of Psychology, Manchester Metropolitan University, Manchester, United Kingdom

²School of Sport, Exercise and Rehabilitation Sciences, and Centre for Human Brain Health, the University of Birmingham, Birmingham, United Kingdom

³Behavioural Brain Sciences Centre, School of Psychology, University of Birmingham, Birmingham, United Kingdom

⁴German Center for Neurodegenerative Diseases, Rostock, Germany

⁵Movement Disorder Unit, Neurology and Neurophysiology Service, Seville Institute of Biomedicine, Virgen del Rocío University Hospital, University of Seville, Seville, Spain

⁶Institute of Neuroscience, Newcastle University, Newcastle upon Tyne, United Kingdom

⁷Department of Neurology, Salford Royal NHS Foundation Trust, Manchester Academic Health Science Centre, University of Manchester, Manchester, United Kingdom

⁸Department of Neurology, Faculty of Medicine, University of Sao Paulo, Functional Neurosurgery Division, Institute of Psychiatry-HCFMUSP, São Paulo, Brazil

⁹Hospital Israelita Albert Einstein, Brain Institute, São Paulo, Brazil

ABSTRACT: Background: There is an urgent need to identify individuals at risk of postural instability and gait difficulties, and the resulting propensity for falls, in Parkinson's disease.

Objectives: Given known relationships between posture and gait and degeneration of the cholinergic pedunculopontine nucleus, we investigated whether metrics of pedunculopontine nucleus microstructural integrity hold independent utility for predicting future postural instability and gait difficulties and whether they could be combined with other candidate biomarkers to improve prognostication of these symptoms.

Methods: We used stereotactic mapping of the pedunculopontine nucleus and diffusion tensor imaging to extract baseline pedunculopontine nucleus diffusivity metrics in 147 participants with Parkinson's disease and 65 controls enrolled in the Parkinson's Progression Markers Initiative. We also recorded known candidate markers of posture and gait changes: loss of caudate dopamine and CSF

β -amyloid 1-42 levels at baseline; as well as longitudinal progression motor symptoms over 72-months.

Results: Survival analyses revealed that reduced dopamine in the caudate and increased axial diffusivity in the pedunculopontine nucleus incurred independent risk of postural instability and gait difficulties. Binary logistic regression and receiver operating characteristics analysis in 117 participants with complete follow-up data at 60 months revealed that only pedunculopontine nucleus microstructure provided more accurate discriminative ability for predicting future postural instability and gait difficulties than clinical and demographic variables alone.

Conclusion: Dopaminergic and cholinergic loss incur independent risk for future postural instability and gait difficulties, and pedunculopontine nucleus microstructure can be used to prognosticate these symptoms from early Parkinson's disease stages. © 2020 The Authors.

This is an open access article under the terms of the Creative Commons Attribution License, which permits use, distribution and reproduction in any medium, provided the original work is properly cited.

***Corresponding author:** Dr. Nicola Ray, Department of Psychology, Manchester Metropolitan University, Brooks Building, 53 Bonsall Street, Manchester M15 6GX, UK; E-mail: n.ray@mmu.ac.uk

Relevant conflicts of interests/financial disclosures: M.S. received meeting honoraria from UCB as well as conference expenses from Medtronic, Bial and Abbvie. The other authors have nothing to disclose.

Funding agencies: The Parkinson's Progression Markers Initiative is sponsored and partially funded by the Michael J. Fox Foundation for Parkinson's Research. Other funding partners include a consortium of industry players, nonprofit organizations, and private individuals. Additional funding to support the current analysis was provided by the Wellcome Trust.

Received: 20 September 2019; **Revised:** 24 February 2020; **Accepted:** 25 February 2020

Published online 13 May 2020 in Wiley Online Library (wileyonlinelibrary.com). DOI: 10.1002/mds.28051

Movement Disorders published by Wiley Periodicals, Inc. on behalf of International Parkinson and Movement Disorder Society.

Key Words: Parkinson's disease; Pedunculopontine nucleus; Postural instability and gait difficulties; prognostic markers

Postural instability and gait disturbance (PIGD) and the resulting increase in falls is associated with a more pernicious disease course in Parkinson's disease (PD), with rapid development of dementia,¹ greater disability,² and early mortality.³ PIGD and falls tend not to respond well to dopamine-replacement medications, but virtual-reality training and nondopaminergic pharmacological interventions have shown early promise.⁴ However, their clinical impact will depend on timely and tailored interventions. As such, there is an urgent need to understand the neural mechanisms that underpin these symptoms and to develop the means to identify individuals at risk.

Longitudinal observational studies have revealed that future postural and gait impairments in PD can be predicted at very early disease stages using dopamine transporter (DAT) imaging of the caudate and measurement of cerebrospinal fluid (CSF) β -amyloid 1-42.^{5,6} Identification of these candidate biomarkers raises the potential that individuals at risk of PIGD can be identified even at very early disease stages, thereby enabling the development of tailored, preventive interventions to mitigate these symptoms. However, taking lessons from cognitive biomarker research,⁷ predicting PIGD with the level of accuracy necessary for clinical trials will depend on our ability to provide a multimodal combinatorial biomarker that reflects the multiple underlying pathophysiological pathways of these symptoms.

There is now strong evidence that loss of brainstem cholinergic neurons, originating in the pedunculopontine nucleus (PPN), plays a significant role in the development of PIGD symptoms. Studies consistently report that cholinergic PPN lesions in primates cause significant PIGD.^{8,9} In humans, *in vivo* cholinergic positron emission tomography (PET) imaging reveals that people with PD with a history of falls—which are more prevalent in people with PIGD¹⁰—have significantly decreased thalamic cholinergic innervation (a major component of which originates in the PPN).¹¹ In addition, the now well-recognized link between PIGD and cognitive decline in PD¹² is suggested to reflect a common underlying pathology of these symptoms originating in the cholinergic neurons of the nucleus basalis of Meynert (nbM).¹³ Thus, the cholinergic contribution to PIGD progression is likely to be driven directly by motor pathways that include the PPN and may also be mediated by cognitive changes following nbM loss. However, to our knowledge, no studies have been conducted in humans to determine the specific contributions of these regions to PIGD in PD.

In vivo structural image analysis of the nbM is now possible via precision, subregional stereotactic mapping developed from postmortem histology and magnetic

resonance.¹⁴ These methods have revealed the spatio-temporal patterns of nbM atrophy in Alzheimer's disease¹⁴ and were recently shown to predict the onset of cognitive decline in early PD.^{15,16} Currently, however, no established imaging method to measure the structure of the PPN exists. Yet such a measure would provide a critical investigative tool to understand the causes of PIGD symptoms and to intervene in their development.

Recently, a stereotactic map of the PPN was developed to improve targeting of the nucleus for deep brain stimulation surgery for dopamine-unresponsive PIGD symptoms.¹⁷ Although automated segmentation of gray and white matter in the brainstem using standard procedures is not accurate, making volumetry of the PPN technically difficult because of its brainstem location, it remains possible that metrics of microstructural integrity provided by diffusion tensor imaging (DTI) would be informative to further understand the neuropathology of PIGD symptoms. Indeed, DTI of the substantia nigra and nbM have revealed microstructural changes in these regions that reflect progression of motor and nonmotor PD symptoms.^{16,18}

In the current study, we combine precision stereotactic mapping of the PPN with DTI to test the hypothesis that microstructural integrity in this region can predict future PIGD symptoms in PD. Given previous suggestions that the nbM may be an important structure for PIGD,¹³ we will also explore whether the nbM microstructure can predict PIGD. Because the PPN microstructure, caudate DAT, and CSF β -amyloid 1-42 concentrations reflect different underlying pathologies, we expect that the PPN microstructure will provide additive prediction of PIGD symptoms over that provided by caudate DAT and/or CSF β -amyloid 1-42 concentrations. As such, we additionally test the prediction that there will be utility in combining these candidate biomarkers to improve prognostication of PIGD in PD.

Methods

Study Design

The Parkinson's Progressive Marker's Initiative (PPMI) is a longitudinal, multicenter study to assess the progression of clinical features, imaging, and biological markers in patients living with PD and healthy controls. It is a public-private partnership funded by the Michael J. Fox Foundation for Parkinson's Research and funding partners, a full list of which can be found at <https://www.ppmi-info.org/about-ppmi/who-we-are/study-sponsors/>.

To enroll in the study, participants with PD must have had a diagnosis for 2 years or less at the screening visit and be at Hoehn and Yahr stages I or II at the baseline visit. Additional inclusion criteria for the PPMI database are described in detail in the PPMI study documents available at <http://www.ppmi-info.org/data>. For up-to-date information on the study, visit www.ppmi-info.org.

Participants

Participants selected from the PPMI for the current study were all those with coregistered T₁-weighted and diffusion-weighted magnetic resonance imaging (MRI) available at baseline, along with at least baseline Movement Disorder Society-UPDRS (MDS-UPDRS) scores. There were 147 participants with PD and 65 control participants.

Clinical, Dopamine Imaging, and CSF Assessments

Following Stebbins and colleagues,¹⁹ PIGD, tremor, rigidity, and bradykinesia symptoms were measured via the UPDRS. These were recorded longitudinally, with data available from baseline, 3, 6, 9, 12, and then 6 monthly intervals up to 72 months. To determine whether PPN diffusivity predicts more serious PIGD, a PIGD endpoint was defined as PIGD UPDRS score > 5. This threshold was chosen because it required at least 1 of the 5 items to have been scored at least 2, reflecting symptoms of a frequency or intensity that are sufficient to cause a modest impact on function. Because of the instability of PIGD scores in early disease, participants meeting this threshold within the first year were required to also have PIGD scores > 5 in subsequent years to be defined as having PIGD. For the same reason, we have chosen not to classify patients by PIGD or tremor-dominant “phenotypes.” This threshold identified ~18% of the sample with more severe PIGD over follow-up.

Endpoints were also defined for tremor, bradykinesia, and rigidity. We tailored these so that ~18% of the PD group met the endpoints, thereby ensuring similar power in statistical tests evaluating risk of each of these symptom types (described Statistical Analysis). The UPDRS thresholds that met this condition were as follows: tremor ≥ 14, rigidity ≥ 11, and bradykinesia ≥ 24.

CSF collection was available in 142 of the PD participants with DTI and was performed as described in the PPMI biologics manual (<http://www.ppmi-info.org/>). CSF β -amyloid 1-42 concentrations were analyzed at the University of Pennsylvania according to the methods in Kang and colleagues.²⁰

All subjects also had DAT imaging at baseline acquired using I-123 Ioflupane single-photon emission computed tomography. The images were centrally reconstructed, attenuation corrected, and caudate and putaminal binding ratios were calculated with reference to DAT counts in the occipital lobe via a standardized

volume of interest template for extraction of regional count densities (<http://www.indd.org/>).

Regions of Interest

PPN

The PPN is the primary area of interest in this study, and diffusion metrics in this region were accessed via a mask created using the methods described in ref. 17. Briefly, postmortem MRI was performed on the brain of a 66-year-old woman without parkinsonism or cognitive decline. Following autopsy, the brain was fixed, dehydrated, serially sectioned, and Nissl stained.²³ Light and darkfield microscopy was used to enhance contrast and perform the segmentation of the nuclear boundaries of the PPN, creating a mask of the entire PPN region. Following digitization, the images were 3-dimensionally registered with the postmortem MRI, and the PPN mask transformed to MNI space via transforms generated following normalisation of the postmortem MRI to MNI space.²⁴

NbM

Given the previous clinical and animal lesion studies showing a relationship between the nbM and PIGD deficits, we also extracted diffusion metrics from a basal forebrain region of interest (ROI), created as described in ref. 14. In brief, the map was derived from combined postmortem MRI and subsequent histological preparation of a brain specimen of a 56-year-old male who had died without any evidence of cognitive decline or psychiatric illnesses. Cerebral MRI scans were performed in situ. Cholinergic nuclei were identified and delineated on digital pictures of the stained brain slices, then manually transferred from the digital pictures into the corresponding magnetic resonance slices. Transformation of the delineations from the space of the dehydrated brain into the space of the in situ brain scan was performed using a high-dimensional nonlinear registration between the 2 brain scans²⁵ before final transformation from in situ space into MNI space using diffeomorphic anatomical registration through exponentiated lie algebra (DARTEL). The stereotactic cholinergic basal forebrain map distinguishes different cholinergic subdivisions. In the current article, we retained the ROI corresponding to the nbM.

Two additional ROIs were used as controls: a whole gray matter (GM) mask created from binarized images of GM segmentations produced as part of the DARTEL procedure, used to control for more widespread changes to brain diffusivity. In addition, to control for the potential contamination of the PPN ROI by nearby white matter, we drew a circular ROI in the corticospinal tract (CST), adjacent to the PPN mask, for use as a nuisance variable in statistical tests.

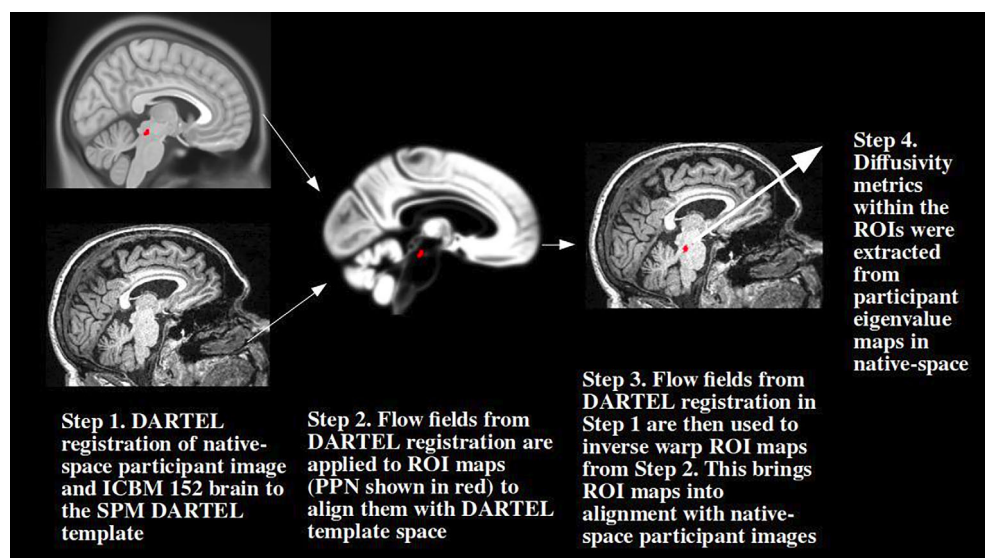


FIG. 1. Preprocessing workflow. T1-images and the MNI space ICBM152 brain¹⁴ were DARTel registered. MNI-space ROI masks were transformed into average template space and then inverse transformed into native space. PPN, pedunculo pontine nucleus; ROI, region of interest. [Color figure can be viewed at wileyonlinelibrary.com]

MRI Processing

Diffusion-weighted images were preprocessed by the PPMI study team according to the pipeline described in <http://www.ppmi-info.org/wp-content/uploads/2011/12/DTI-processing-Pipeline3.pdf>. This pipeline produces eigenvalue (λ) maps coregistered to T1 anatomical images, which we downloaded from the PPMI. The workflow employed following this is illustrated in Figure 1. First, to transform MNI-space ROI images (described in Regions of Interest) to native space, T1-images were first segmented into separate gray, white, and CSF tissue compartments for DARTel initialization, implemented in SPM12 (<https://www.fil.ion.ucl.ac.uk/spm/software/spm12/>). DARTel performs a diffeomorphic algorithm for intersubject registration, producing individual flow field maps (which parameterize the deformation of the images) as well as average gray and white matter templates. The MNI-space ICBM152 brain²¹ was then DARTel registered to the template separately, and the resultant flow field was used to transform the MNI-space ROIs into the average template space. Finally, the participants' individual flow fields were used to inverse transform the warped ROI images into participant native space. All warps of the ROI maps used nearest-neighbor interpolation. Each ROI was visually checked by an expert observer for alignment with the PPN (author N.J.) and nbM (author N.J.R.) regions.

In addition, the current gold-standard method for locating the PPN involves using atlas-based coordinates, described by Zrinzo and colleagues.²² To confirm our methods, we tested whether the transformed PPN ROI masks overlapped with the coordinates provided in Zrinzo and colleagues,²² in

a smaller selection of 20 images. Figure 2 illustrates this check, showing a representative image from a single participant with the PPN mask overlaid along with the atlas-based coordinates of the rostral pole of the PPN.

Finally, mean eigenvalues from the ROIs were extracted from each of the 3 eigenvalue images, and mean, axial (along the principal axis), and radial (perpendicular to the principal axis) diffusivity (mD, aD, rD, respectively) were calculated according to the following: $mD = (\lambda_1 + \lambda_2 + \lambda_3) / 3$; $aD = \lambda_1$; $rD = (\lambda_2 + \lambda_3) / 2$. Please note that we have not utilized the fractional anisotropy maps available in the PPMI for the current analysis. We avoided this because changes in fractional anisotropy are extremely difficult to interpret in GM (degeneration of

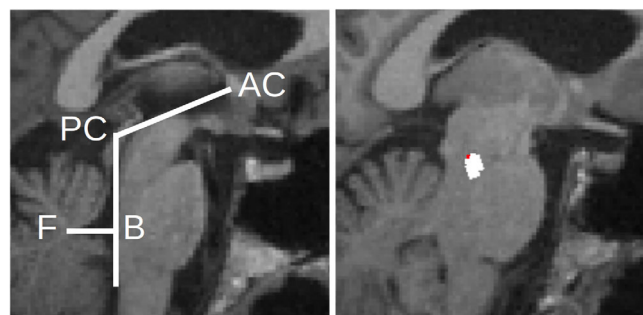


FIG. 2. Atlas-based localization of the pedunculo pontine nucleus. Localization of the pedunculo pontine nucleus using the current automatic method (voxels are labeled in white following procedure outlined in Fig. 1). The voxels identified as belonging to the pedunculo pontine nucleus were then confirmed using the manual atlas-based method described in Zrinzo and colleagues²² (red point represents the rostral pole of the atlas coordinates provided in that article). AC, anterior cingulate; PC, posterior cingulate. [Color figure can be viewed at wileyonlinelibrary.com]

neurons oriented in different directions would cause a paradoxical increase in fractional anisotropy, whereas degeneration of neurons oriented in the same direction would have the opposite effect), and this may be particularly true in a region such as the PPN that is expected to be heavily myelinated.

Statistical Analysis

Statistical analyses were conducted in SPSS Statistics version 22 (IBM, Armonk, NY) and R (<http://www.R-project.org/>; R Foundation for Statistical Computing, Vienna, Austria).

Baseline Demographics, Clinical Scores, Diffusivity, DAT, and CSF Measures

Analyses of variance and post hoc Tukey tests were used to compare demographics, clinical measures, diffusivity metrics, mean caudate DAT, and CSF β -amyloid 1-42 metrics between the controls and PD participants who did/did not develop more severe PIGD. Subsequent univariate tests were conducted for diffusivity metrics that showed between-group differences, controlling for age, UPDRS part III scores and whole GM and CST diffusivity. Note that diffusivity metrics were matched in each analysis, for example, comparisons/correlations involving PPN aD controlled for whole brain aD and CST aD.

Survival Analysis

Cox proportional hazards regression analyses were used to test the hypothesis that development of more severe PIGD can be predicted by PPN microstructure measured at the time of PD diagnosis. None of the variables included violated collinearity assumptions. Time to severe PIGD was calculated as the number of months since study enrolment until the PIGD threshold (PIGD >5) was reached. One participant already meeting this threshold at baseline was excluded from this analysis. The prediction of severe tremor, rigidity, and bradykinesia were also evaluated in separate Cox regressions.

Control variables considered for inclusion in the analysis were age, Montreal Cognitive Assessment, UPDRS part III, baseline PIGD, and sex. This clinical and demographics only model was run as a first step, and all predictors surviving $P < 0.2$ were retained for the full model, with sex and Montreal Cognitive Assessment not meeting this criterion. Diffusivity metrics from each ROI were then added to the model separately (with whole GM and CST diffusivity added as additional control variables).

Caudate DAT and CSF β -amyloid 1-42 concentrations were subsequently added to the clinical, demographics, and diffusivity models to determine their

shared and/or unique predictive relationships with diffusivity metrics for PIGD.

Binary Logistic Regression and ROC Analysis

In a smaller sample of participants with full data available at the 60-month follow-up visit ($N = 117$), binary logistic regression was used to model the predictive relationships between PIGD and candidate markers along with clinical and demographic variables. Using the pROC²⁶ package in R, ROC curves were constructed from the predicted values from a demographics and clinical characteristics-only model and from models including candidate markers together or in isolation. Areas under the curves (AUC) were compared with the DeLong method,²⁷ with the prediction that inclusion of biomarkers would provide more accurate discriminative ability for predicting PIGD than the clinical and demographic-only model.

Correction for Multiple Comparisons

All analyses are presented with uncorrected P values, and those surviving false discovery rate correction for number of diffusivity metrics and number of ROIs included in the analysis are noted in the text.

Results

Clinical, Demographic, and Diffusivity Characteristics at Baseline in Controls, People with PD Who Develop PIGD During Follow-Up Visits, and People with PD Who Do Not Develop PIGD at Follow-Up

A total of 27 (18.4%) participants with PD developed severe PIGD during the 72-month follow-up period. One-way analysis of variance and post hoc Tukey tests revealed that the PD participants who developed PIGD during the follow-up period were older and had worse UPDRS part III scores at baseline than those who did not develop PIGD. This group was also found to have greater aD in the PPN when compared with both controls and participants with PD who did not develop PIGD (statistics reported in Table 1).

The latter finding survived false discovery rate correction for 2 (ROI: nbM and PPN) \times 3 (diffusivity metrics: aD, mD, and rD) multiple comparisons, and univariate analyses revealed that PPN aD was significantly greater in the PD participants who did develop PIGD (compared with those who did not) even after controlling for age, sex, UPDRS part III scores, Montreal Cognitive Assessment scores, and CST aD and whole GM aD ($F = 10.57$, $P = 0.001$).

TABLE 1. Demographics, clinical characteristics, and diffusivity metrics

	Participants with PD and PIGD <6 During Follow-Up (N = 120, Female = 46)		Participants with PD and PIGD ≥6 During Follow-Up (N = 27, Female = 8)		Controls (N = 65, Female = 22)	
	Mean	SD	Mean	SD	Mean	SD
Age, y	60.49	9.32	65.17	9.05	60.51	10.66
Education, y	15.34	3.12	14.74	2.75	15.23	3.06
MDS-UPDRS part III	19.67	8.10	25.19	11.26	0.57	1.31
MoCA	27.62	2.07	27.15	2.29	28.17	1.14
Caudate DAT	1.94	0.49	1.62	0.60	2.71	0.43
CSF β-amyloid 1-42 (pg/mL)	865.70	324.57	781.31	316.87	961.42	467.41
PPN aD	1.21	0.094	1.28	0.10	1.23	0.094
PPN mD	0.69	0.05	0.71	0.06	0.70	0.06
PPN rD	0.41	0.06	0.41	0.06	0.44	0.07
nbM aD	1.28	0.13	1.29	0.08	1.25	0.13
nbM mD	1.01	0.13	1.03	0.09	0.99	0.11
nbM rD	0.87	0.14	0.90	0.10	0.86	0.11
Caudal SN aD	1.05	0.11	1.12	0.11	1.03	0.10
Caudal SN mD	0.74	0.10	0.77	0.08	0.72	0.10
Caudal SN rD	0.58	0.09	0.60	0.07	0.56	0.11

Note: Bold values indicate significantly different from PD patients who did not develop PIGD at $P < 0.05$ corrected.

PD, Parkinson's disease; PIGD, postural instability and gait difficulties; SD, standard deviation; UPDRS, Unified Parkinson's Disease Rating Scale; MoCA, Montreal Cognitive Assessment; DAT, dopamine transporter; CSF, cerebrospinal fluid; PPN, pedunculo-pontine nucleus; aD, aD, axial diffusivity; mD, mean diffusivity; rD, radial diffusivity; nbM, nucleus basalis of Meynert; SN, substantia nigra; MDS-UPDRS, Movement Disorder Society-Unified Parkinson's disease Rating Scale.

More severe tremor, rigidity, and bradykinesia developed in 28, 26, and 31 patients with PD, respectively. There was some overlap between these groups (8, 14, and 15 patients with more severe tremor, rigidity, and bradykinesia also had more severe PIGD). However, diffusivity metrics were not different in those developing these symptoms versus those who did not ($T < 1.62$, $P > 0.10$).

Do Diffusivity Characteristics Incur Risk for PIGD Independently from Clinical and Demographic Markers for PIGD: Survival Analysis

Clinical and demographic variables (age, baseline PIGD, and total UPDRS part III scores) were entered into Cox regression models along with diffusivity metrics in the nbM and PPN. Whole GM and CST diffusivity were also entered as control regions. NB, the 3 diffusivity metrics (aD, mD, and rD) extracted from the 2 ROIs (nbM and PPN) were entered into separate models, and therefore results are corrected for 3×2 multiple comparisons.

PPN aD was the only metric to be associated with significant independent risk of developing PIGD (PPN aD: Wald = 9.32, $P = 0.002$ [survives false discovery rate correction for multiple comparisons]). For the nbM and all other diffusivity metrics, Wald < 0.90 and $P > 0.35$. To determine the specificity of PPN aD for predicting PIGD, we repeated the survival analysis to predict tremor, rigidity, and bradykinesia. None of

these were found to be predicted by PPN aD (Wald < 1.81, $P > 0.18$).

Do Diffusivity Characteristics Incur Risk for PIGD Independently from Clinical, Demographic, and Other Candidate Markers for PIGD: Survival Analysis

Given the previous results, the analyses that follow were not performed for diffusivity metrics in the nbM.

Caudate DAT, but not putamen DAT, also predicted future PIGD (caudate: Wald = 7.63, $P = 0.006$; putamen: Wald = 0.72, $P = 0.40$). With PPN aD and caudate DAT entered together (as well as CST and whole GM aD), PPN aD (Wald = 6.60, $P = 0.01$) and caudate DAT (Wald = 3.11, $P = 0.05$) explained the significant independent risk of PIGD.

CSF β-amyloid 1-42 did not reach significance for predicting the risk of PIGD in a model that did not include caudate DAT or PPN aD (Wald = 2.62, $P = 0.11$), and both caudate DAT (Wald = 4.75, $P = 0.03$) and PPN diffusivity (Wald = 5.81, $P = 0.01$) continued to predict PIGD when entered with CSF β-amyloid 1-42.

Does PPN Diffusivity and/or Other Candidate Markers of PIGD Improve Discriminative Ability for Predicting PIGD over Demographic and Clinical Variables: Binary Logistic Regression

In a sample of participants with follow-up data available at 60 months (N = 117), a binary logistic

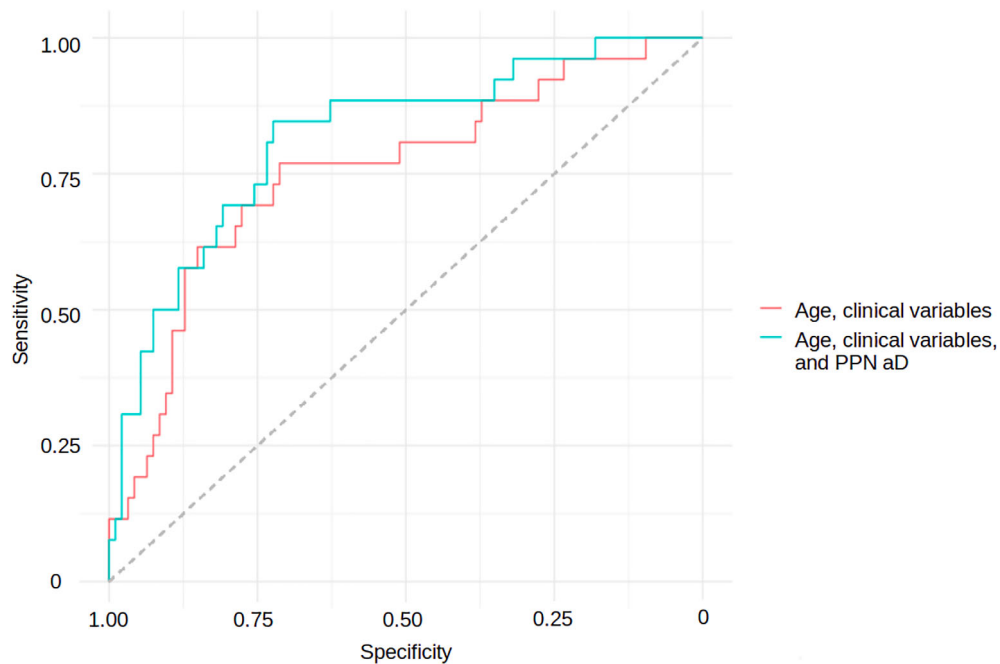


FIG. 3. Receiver operating characteristic curves of predictive models for postural instability and gait disturbance. Receiver operating characteristic curve for a demographics and clinical characteristics-only model is shown in pink. The addition of PPN aD to the demographics and clinical characteristics model is shown in blue. aD, axial diffusivity; PPN, pedunculopontine nucleus. [Color figure can be viewed at wileyonlinelibrary.com]

regression including demographic and clinical variables, as well as both PPN aD and caudate DAT confirmed that PPN aD independently predicted severe PIGD (Wald = 6.93, $P = 0.008$), whereas caudate DAT marginally missed significance (Wald = 3.53, $P = 0.06$). The AUC for a ROC curve computed from predicted values of a binary logistic regression that included only demographic and clinical variables was 0.74 (95% confidence interval, 0.64–0.87). Improvements to this provided by PPN aD (AUC, 0.82; 95% confidence interval, 0.72–0.91) were significant ($z = 1.8$, $P = 0.03$; Fig. 3). The addition of the caudate DAT to the demographic and clinical-only model (AUC: 0.78, CI: 0.66–0.89) was not significant ($z < 0.88$, $P > 0.19$), and the model that included both the PPN aD and caudate DAT (AUC, 0.82; 95% confidence interval, 0.72–0.92) was not significantly better than the model including demographic and clinical variables and PPN aD ($z = 0.48$, $P = 0.68$).

Discussion

Our study shows that microstructural changes in the PPN are associated with an increased risk for the development of PIGD symptoms in PD and have discriminative ability for predicting PIGD within 5 years, even at very early disease stages. This finding is specific to the symptoms of PIGD (development of significant tremor, rigidity, and bradykinesia symptoms were unrelated to

PPN diffusivity) and was specific to the PPN (microstructural changes in the nbM did not incur risk for PIGD symptoms). The latter finding implies that degeneration in the PPN and its relationship with future PIGD does not reflect a general PD-related decline in cholinergic subcortical nuclei and supports the suggestion that pathology of the PPN can cause PIGD in PD. This raises the potential that measures of PPN microstructure could be used to stratify patients to enable tailored and preventive interventions for gait and balance deficits and for future clinical trials.

The anatomical and functional specificity of this finding for the PPN and PIGD, respectively, is consistent with our current understanding of this region's role in normal walking and balance. In animal models, PPN lesions are sufficient to induce gait deficits, and stimulation of the PPN results in locomotion.^{8,9} Depth recordings from the PPN in humans reveal modulated single-unit firing during imagined walking²⁸ and enhanced α -band oscillations during stepping in place.²⁹ Lau and colleagues²⁸ provide evidence that the PPN influences gait in ways that extend beyond “pattern generation,” including motor planning and adaptation. The methods reported in the current article will enable further investigation of the role of the PPN in these skills.

The PPN is a neurochemically heterogeneous structure, containing gamma aminobutyric acid (GABA)ergic, glutamatergic, and cholinergic populations.³⁰ The cholinergic neurons of the PPN seem to be particularly relevant for PIGD and falls as demonstrated by the gait deficits

produced by targeted cholinergic lesions of the PPN in primates and rodents.⁸ Positron emission tomography with cholinergic ligands and pathological data has shown relationships between PPN-thalamic cholinergic innervation and PIGD and falls in PD.¹¹ Although the current findings make no distinction between neurochemical subpopulations of PPN neurons, taken with the previous findings, we can speculate that PPN aD reflects, at least in part, degeneration of PPN-thalamic cholinergic projections.

As expected, given previous literature,⁵ we found that the risk of PIGD was increased by low caudate DAT at baseline. This relationship was independent from the relationship between PPN aD and future PIGD, implying there are distinct dopaminergic and cholinergic contributions to the risk of developing these symptoms. There is a known link between PIGDs—specifically freezing of gait—and frontal executive functions,³¹ and the dependence of these on caudate dopamine is well documented. It is reasonable therefore to speculate that the link between caudate dopamine depletion and PIGD is mediated by impaired executive function. Similarly, a previous study using DTI with tractography revealed that freezing of gait was associated with reduced connectivity between the PPN and the frontal cortex, which was in turn associated with impaired executive function.³² As such, combining the methods reported here to study these links could reveal the multiple pathologies that underpin the failure of the motor and/or non-motor networks to support posture and gait in PD.

In follow-up analyses, only PPN aD significantly increased accuracy of a predictive model for PIGD beyond clinical and demographic variables alone. These results indicate that although there is a clear relationship between dopamine deficiency and PIGD,⁵ it may not discriminate between people who do/do not develop these symptoms. Conversely, cholinergic loss develops more heterogeneously in PD, and the current findings indicate that this variability provides greater predictive utility for the symptoms that are underpinned by this loss.

The corticopetal cholinergic system originating in the nbM has been linked to gait speed and falls,^{11,33} but the risk of PIGD was not predicted by nbM diffusivity in the current report. It has been suggested that gait changes and increased falls risk follow cognitive deterioration, particularly in executive function and attention,³⁴ and that degeneration in the nbM is the principal underlying factor.¹³ We are currently investigating whether datasets with more fine-grained cognitive, gait, and postural measures (<http://bam-ncl.co.uk/our-work/studies/icicle-gait/>) than provided by the PPMI are informative for the role of the nbM in these abilities.

Finally, we did not observe a relationship between CSF β -amyloid 1-42 concentrations at baseline and risk of PIGD. Yet, previous data has consistently reported a

relationship between PIGD severity and CSF β -amyloid levels,^{5,6} as well as neocortical β -amyloid deposition measured with PET.³⁵ It is possible that the relationship between CSF β -amyloid 1-42 concentrations and PIGD symptoms is more readily detected using methods that characterize PIGD severity using more fine-grained, continuous measures rather than when PIGD is expressed as a dichotomous variable as required by survival and binary regression analyses. As such, the lack of a predictive relationship reported here between CSF β -amyloid 1-42 concentrations and UPDRS PIGD >5 should be viewed as a limitation of these methods rather than evidence that a relationship does not exist.

Some caveats to the current study must be acknowledged. First, volumetry of the PPN is difficult because of the requirement to accurately segment white matter and GM in this region. As such, we have not corrected for partial volume effects. However, our aim was to provide a measure of structural change in the region that may have utility for understanding and predicting PIGD in PD. Therefore, whether our prognostic marker reflects micro- and/or macro-structural changes is not a focus of the current article. That said, the application of more accurate segmentation procedures for brainstem structures are warranted. Similarly, the seeming specificity of the marker for PPN aD, rather than mD or rD, is currently open to interpretation. The current analysis is not able to determine the specific neurodegenerative process that leads to increased aD. However, we are continuing to investigate the relationship between the PPN and PIGD using alternative DTI metrics³⁶ that will enable us to address these additional questions.

In addition, we defined PIGD >5 as the end point for our predictive analyses as it allowed us to distinguish individuals who are beginning to experience functional limitation attributable to at least 1 PIGD marker. However, it is not clear from the current study whether this is the most sensitive end point to use. It is also not clear whether there is a linear relationship between PPN degeneration and the emergence of PIGD symptoms. Future work could aim to explore these relationships to determine the point at which PPN degeneration becomes risky for developing PIGD as well as whether longitudinal progression of PPN degeneration is more informative than cross-sectional baseline data for predicting PIGD. Finally, it must also be noted that PIGDs are overrepresented in atypical parkinsonian disorders,³⁷ and it is therefore possible that patients developing PIGD in the current sample may later be diagnosed with atypical parkinsonian disorders.

In conclusion, stereotactic mapping alongside DTI of the PPN can be used to prognosticate PIGD in PD. The relationship between baseline PPN micro-structure and future PIGD was independent from the

relationship between caudate dopamine deficiency and future PIGD, implying that there are distinct dopaminergic and cholinergic contributions to the risk of developing these symptoms. It is now necessary to further investigate how measures of PPN and dopaminergic integrity could be combined in algorithms to predict the onset of particular components, or complications, of PIGD, such as freezing of gait or falls. ■

References

- Burn DJ, Rowan EN, Allan LM, Molloy S, O'Brien JT, McKeith IG. Motor subtype and cognitive decline in Parkinson's disease, Parkinson's disease with dementia, and dementia with Lewy bodies. *J Neurol Neurosurg Psychiatry* 2006;77:585–589.
- Post B, Merkus MP, de Haan RJ, Speelman JD, CARPA Study Group. Prognostic factors for the progression of Parkinson's disease: a systematic review. *Mov Disord* 2007;22:1839–1851; quiz 1988.
- Bäckström D, Granäsén G, Domellöf ME, et al. Early predictors of mortality in parkinsonism and Parkinson disease: A population-based study. *Neurology* 2018;91:e2045–e2056.
- Mirelman A, Rochester L, Maidan I, et al. Addition of a non-immersive virtual reality component to treadmill training to reduce fall risk in older adults (V-TIME): a randomised controlled trial. *Lancet* 2016;388:1170–1182.
- Kim R, Lee J, Kim HJ, et al. CSF β -amyloid42 and risk of freezing of gait in early Parkinson disease. *Neurology* 2019;92:e40–e47.
- Rochester L, Galna B, Lord S, et al. Decrease in A β 42 predicts dopa-resistant gait progression in early Parkinson disease. *Neurology* 2017;88:1501–1511.
- Schrag A, Siddiqui UF, Anastasiou Z, Weintraub D, Schott JM. Clinical variables and biomarkers in prediction of cognitive impairment in patients with newly diagnosed Parkinson's disease: a cohort study. *Lancet Neurol* 2017;16:66–75.
- Karachi C, Grabli D, Bernard FA, et al. Cholinergic mesencephalic neurons are involved in gait and postural disorders in Parkinson disease. *J Clin Invest* 2010;120:2745–2754.
- Grabli D, Karachi C, Folgoas E, et al. Gait disorders in parkinsonian monkeys with pedunculopontine nucleus lesions: a tale of two systems. *J Neurosci* 2013;33:11986–11993.
- Hiorth YH, Alves G, Larsen JP, Schulz J, Tysnes OB, Pedersen KF. Long-term risk of falls in an incident Parkinson's disease cohort: the Norwegian ParkWest study. *J Neurol* 2017;264:364–372.
- Bohnen NI, Kanel P, Zhou Z, et al. Cholinergic system changes of falls and freezing of gait in Parkinson's disease. *Ann Neurol* 2019;85:538–549.
- Morris R, Lord S, Lawson RA, et al. Gait rather than cognition predicts decline in specific cognitive domains in early Parkinson's disease. *J Gerontol A Biol Sci Med Sci* 2017;72:1656–1662.
- Yarnall A, Rochester L, Burn DJ. The interplay of cholinergic function, attention, and falls in Parkinson's disease. *Mov Disord* 2011;26:2496–2503.
- Kilimann I, Grothe M, Heinsen H, et al. Subregional basal forebrain atrophy in Alzheimer's disease: a multicenter study. *J Alzheimers Dis* 2014;40:687–700.
- Ray NJ, Bradburn S, Murgatroyd C, et al. In vivo cholinergic basal forebrain atrophy predicts cognitive decline in de novo Parkinson's disease. *Brain J Neurol* 2018;141:165–176.
- Schulz J, Pagano G, Fernández Bonfante JA, Wilson H, Politis M. Nucleus basalis of Meynert degeneration precedes and predicts cognitive impairment in Parkinson's disease. *Brain J Neurol* 2018;141:1501–1516.
- Alho ATDL, Hamani C, Alho EJJ, et al. Magnetic resonance diffusion tensor imaging for the pedunculopontine nucleus: proof of concept and histological correlation. *Brain Struct Funct* 2017;222:2547–2558.
- Vaillancourt DE, Spraker MB, Prodoehl J, et al. High-resolution diffusion tensor imaging in the substantia nigra of de novo Parkinson disease. *Neurology* 2009;72:1378–1384.
- Stebbins GT, Goetz CG, Burn DJ, Jankovic J, Khoo TK, Tilley BC. How to identify tremor dominant and postural instability/gait difficulty groups with the movement disorder society unified Parkinson's disease rating scale: comparison with the unified Parkinson's disease rating scale. *Mov Disord* 2013;28:668–670.
- Kang J-H, Irwin DJ, Chen-Plotkin AS, et al. Association of cerebrospinal fluid β -amyloid 1–42, T-tau, P-tau181, and α -synuclein levels with clinical features of drug-naïve patients with early Parkinson disease. *JAMA Neurol* 2013;70:1277–1287.
- Heinsen H, Arzberger T, Schmitz C. Celloidin mounting (embedding without infiltration) - a new, simple and reliable method for producing serial sections of high thickness through complete human brains and its application to stereological and immunohistochemical investigations. *J Chem Neuroanat* 2000;20:49–59.
- Avants BB, Epstein CL, Grossman M, Gee JC. Symmetric diffeomorphic image registration with cross-correlation: evaluating automated labeling of elderly and neurodegenerative brain. *Med Image Anal* 2008;12:26–41.
- Ashburner J, Friston KJ. Nonlinear spatial normalization using basis functions. *Hum Brain Mapp* 1999;7:254–266.
- Mazziotta JC, Toga AW, Evans A, Fox P, Lancaster J. A probabilistic atlas of the human brain: theory and rationale for its development: the International Consortium for Brain Mapping (ICBM). *NeuroImage* 1995;2:89–101.
- Zrinzo L, Zrinzo LV, Tisch S, et al. Stereotactic localization of the human pedunculopontine nucleus: atlas-based coordinates and validation of a magnetic resonance imaging protocol for direct localization. *Brain* 2008;131:1588–1598.
- Robin X, Turck N, Hainard A, et al. pROC: an open-source package for R and S+ to analyze and compare ROC curves. *BMC Bioinformatics* 2011;12:77.
- DeLong ER, DeLong DM, Clarke-Pearson DL. Comparing the areas under two or more correlated receiver operating characteristic curves: a nonparametric approach. *Biometrics* 1988;44:837–845.
- Lau B, Welter ML, Belaid H, et al. The integrative role of the pedunculopontine nucleus in human gait. *Brain J Neurol* 2015;138:1284–1296.
- Fraix V, Bastin J, David O, et al. Pedunculopontine nucleus area oscillations during stance, stepping and freezing in Parkinson's disease. *PLoS ONE* 2013;8:e83919.
- Jenkinson N, Nandi D, Muthusamy K, et al. Anatomy, physiology, and pathophysiology of the pedunculopontine nucleus. *Mov Disord* 2009;24:319–328.
- Amboni M, Cozzolino A, Longo K, Picillo M, Barone P. Freezing of gait and executive functions in patients with Parkinson's disease. *Mov Disord* 2008;23:395–400.
- Fling BW, Cohen RG, Mancini M, Nutt JG, Fair DA, Horak FB. Asymmetric pedunculopontine network connectivity in parkinsonian patients with freezing of gait. *Brain* 2013;136:2405–2418.
- Bohnen NI, Frey KA, Studenski S, et al. Gait speed in Parkinson disease correlates with cholinergic degeneration. *Neurology* 2013;81:1611–1616.
- Allcock LM, Rowan EN, Steen IN, et al. Impaired attention predicts falling in Parkinson's disease. *Parkinsonism Relat Disord* 2009;15:110–115.
- Müller ML, Frey KA, Petrou M, et al. β -Amyloid and postural instability and gait difficulty in Parkinson's disease at risk for dementia. *Mov Disord* 2013;28:296–301.
- Muhlert N, Sethi V, Schneider T, et al. Diffusion MRI-based cortical complexity alterations associated with executive function in multiple sclerosis. *J Magn Reson Imaging* 2013;38:54–63.
- Köllensperger M, Geser F, Seppi K, et al. Red flags for multiple system atrophy. *Mov Disord* 2008;23:1093–1099.